IEEE Photonics Journal
An IEEE Photonics Society Publication

Open Access

Tuneable Dual-Mode Micro-Resonator Associating Photonic Crystal Membrane and Fabry–Perot Cavity

Volume 6, Number 2, April 2014

K. Kusiaku
J.-L. Leclercq
P. Viktorovitch
X. Letartre

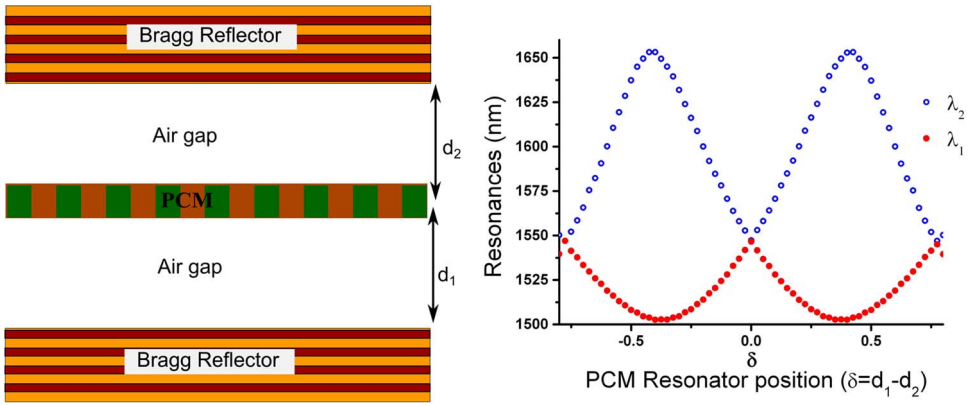

DOI: 10.1109/JPHOT.2014.2306841
1943-0655 © 2014 IEEE

IEEE photonics SOCIETY

IEEE

Tuneable Dual-Mode Micro-Resonator Associating Photonic Crystal Membrane and Fabry–Perot Cavity

K. Kusiaku, J.-L. Leclercq, P. Viktorovitch, and X. Letartre

Université de Lyon, Institut des Nanotechnologies de Lyon (INL), UMR CNRS 5270, Ecole Centrale de Lyon, F 69134 Ecully Cedex, France

DOI: 10.1109/JPHOT.2014.2306841
1943-0655 © 2014 IEEE. Translations and content mining are permitted for academic research only. Personal use is also permitted, but republication/redistribution requires IEEE permission. See http://www.ieee.org/publications_standards/publications/rights/index.html for more information.

Manuscript received January 20, 2014; revised February 10, 2014; accepted February 11, 2014. Date of publication February 19, 2014; date of current version March 3, 2014. Corresponding author: K. Kusiaku (e-mail: koku.kusiaku@cea.fr).

Abstract: We report on a tuneable dual-wavelength micro-resonator with a resonant photonic crystal membrane (PCM) inserted in a vertical Fabry–Perot (FP) cavity. Strong optical coupling between both resonators leads to dual-wavelength resonances. Their energy difference, determined by the overlap of both modes, can be tuned using micro-opto-electro-mechanical systems. Variations in spectral and field overlaps are considered separately with a phenomenological matrix method through, respectively, the FP cavity thickness and the PCM position change. This approach is compared with 2-D finite-difference time-domain simulations in the second case. Periodic evolution of both modes is observed with unsymmetrical amplitude, unlike with the model cause of its approximations.

Index Terms: Photonic crystals, Dual-wavelength micro-resonator, MOEMS.

1. Introduction

Photonic crystal structures offer a unique opportunity of engineering high quality factor and small mode volume nano-cavity for highly integrated optics. Although three-dimensional (3D) photonic crystal presents the major advantage to control light in any direction, most research effort is focused on planar photonic crystal development because of much easier technological fabrication. In this approach, the confinement in the vertical direction is ensured by total internal reflection due to the high index contrast between the photonic crystal membrane (PCM) and its cladding. However, some in-plane guided wave modes suffer from out-of plane coupling with free space modes. Those leaky modes offer an appealing way of extending the planar technology in the vertical direction, provided that we can control the coupling between guided and free-space modes through a multilayer vertical patterning. This approach, so named 2.5D micro-photonics [1], has been successfully experienced to provide vertical switching devices and a low threshold PCM laser sources [2], [3].

In this context, we have recently investigated the coupling between a PCM Bloch mode at the Γ-point of the Brillouin zone and a vertical resonant Fabry–Perot cavity standing mode with the same resonant frequency f_0 [4]. It is worth noticing that a Γ-point Bloch mode can be specifically addressed by a normal incidence beam. Consequently, these two modes may interact, provided that their field overlapping is non-zero. An interesting architecture consists therefore in the insertion of a PCM into a FP cavity (Fig. 1.), in order to control its optical mode coupling with the field

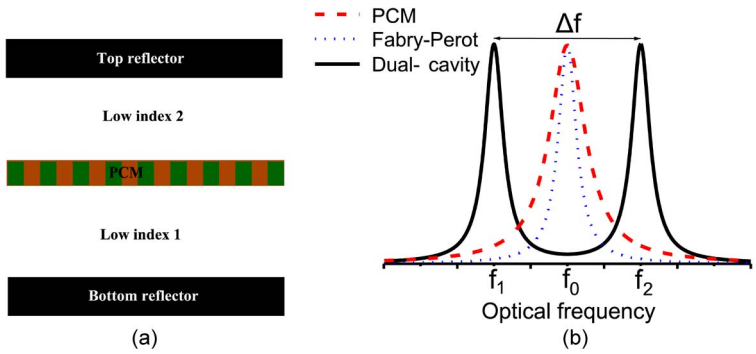

Fig. 1. (a) Schematic view of a coupled PCM and FP cavity system. (b) Representation of the FP, PCM, and hybrid cavity resonances. The dual-mode behaviour results from the coupling between the FP and the PCM modes.

distribution of the standing vertical resonant FP mode. Such system has been found to operate either in weak or strong optical coupling regime when both resonators are tuned [4]. In the last case, the system exhibits two resonant "hybrid modes" symmetrically shifted from f_0, whose energy difference is mainly determined by the overlap between the PCM Γ-point Bloch mode and the FP cavity mode. The resulting dual-wavelength resonant micro-cavity is attractive for various applications involving the interaction of signals with different frequencies, as it can take advantage of resonantly induced enhancement of the field intensity at two wavelengths. This effect has been used previously for non linear effects like harmonic generation [5], [6]. Low threshold Raman micro-lasers have been also demonstrated using two resonant modes, one for the pump signal and one for the laser one, in a PCM cavity [7]. Specifically, we aim in this project at developing a vertical emission dual-wavelength compact micro-laser with application in terahertz wave generation [8], [9].

As a part of the FP cavity can be constituted by air gaps (Fig. 1.), a vertical tuneable dual-wavelength micro-cavity can be produced using micro-opto-electro-mechanical systems (MOEMS), in which some of the membranes are freely released [10]–[13]. The air gaps thicknesses can be increased (or decreased) by deflecting suspended membranes with integrated electrostatic actuators. In our case, an electrostatic actuator can be used to tune either the FP cavity thickness or the PCM position in the cavity as further detailed. This would lead to control the coupling between the FP and PCM modes.

In this paper, we demonstrate numerically the tuneability of the hybrid resonant modes by using a phenomenological matrix transfer approach [1] and a rigorous finite difference time domain (FDTD) [14] simulations. Basic design rules and characteristics of the coupled PCM and FP cavity system are summed up and the tuneablility options are discussed. Next, we consider a simple phenomenological model approach which has been shown to be in good agreement with numerical FDTD [1], [4]. It combines coupled mode theory and matrix transfer analysis where the dual-wavelength micro-cavity is seen as a simple resonator embedded in an air FP cavity formed by two quarter-wave high index contrast Bragg reflectors. In the case of numerical simulation, only the effect of the PCM displacement will be considered with "*ab initio*" 2D-FDTD calculations. Two designs depending on the FP cavity structure are presented. First, two quarter-wave Bragg reflectors FP cavity is considered. Secondly and in order to improve the device compactness, a FP cavity formed between a Bragg reflector and a broadband PCM reflector [15], [16] based design is presented.

2. Design

A schematic view of the coupled PCM and FP cavity system is shown in Fig. 1(a). It consists in a PCM resonator enclosed in a vertical FP cavity formed by two highly reflective mirrors. The PCM is surrounded by a low index medium gap on both sides. In the prospect of a tuneable device, one or both gap(s) must be in air to provide suspended membrane(s) which can be actuated using an electrostatic force.

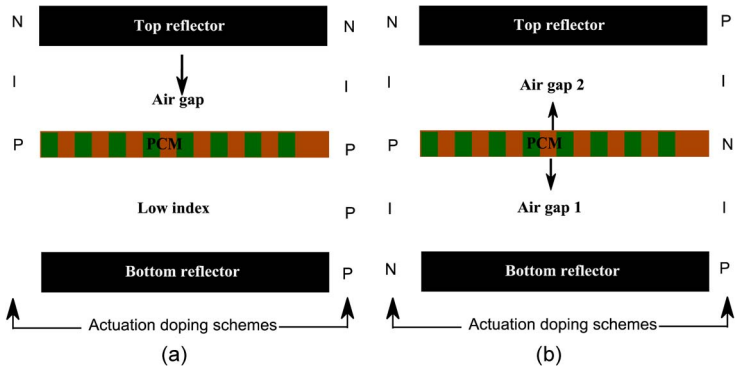

Fig. 2. Schematic view of a coupled PCM and FP cavity system with electrostatic actuation doping scheme illustrations for (a) the top mirror actuation and (b) the PCM actuation.

The PCM could be either 1D or 2D sub-wavelength resonant grating membrane. The presence of leaky resonant guided wave modes in a PCM was long understood [17], [18]. Those modes, located above the so-called light line, appear in the transmission/reflection spectra of a beam propagating towards the PCM with an incident angle corresponding to the in-plane wave-vector of the PCM Bloch mode. We particularly focus on the Γ-point Bloch modes, as mentioned earlier, corresponding to a normal incidence to the PCM plane. These modes can interact with free space plane wave with a coupling coefficient $1/\tau_c$, where τ_c is the photon lifetime in the membrane. It must be pointed out here that the PCM must be designed to insure a specular reflection because every higher order diffracted modes will not contribute to the coupling between the PCM and FP modes.

Let us consider the design of Fig. 1(a) where the PCM and the FP cavity are supporting modes with the same frequency f_0 as illustrated on Fig. 1(b). We have demonstrated [4] using coupled mode theory analysis that weak or strong coupling regime can occur depending on the ratio τ_c/τ_{FP}, where τ_{FP} is the FP cavity decay time. In the strong coupling regime, the system exhibits two hybrid modes at frequencies f_1 and f_2, symmetrically shifted from f_0 [Fig. 1(b)]. The frequency difference $\Delta f = |f1 - f2|$ depends on the coupling strength which is linked to the spectral and spatial overlaps of the FP cavity and the PCM resonator optical modes. Let us notice here that the strong coupling regime condition is always satisfied for $\tau_c/\tau_{FP} \leq 1$. Hence, this condition will be adopted for both phenomenological and numerical FDTD simulations.

Electrostatic actuation can be used to move suspended parts of the micro-cavity, for instance the top mirror or the PCM membrane, in order to monitor the coupling strength. As mentioned earlier, and in addition to the strong coupling regime condition, the coupling requires spectral and field overlaps between the PCM and the FP cavity modes. The starting point of the tuneability schemes is to modify such overlaps in order to vary the coupling strength.

First, a control of the FP cavity thickness can be used to vary its resonance frequency, therefore modulating the spectral overlap between the PCM and FP modes, while maintaining the later resonance frequency close to the central frequency f_0. This can be done by integrating a simple "pin" diode hetero-junction between the top mirror and the PCM resonator membrane as shown in Fig. 2(a). When biasing the junction, an electrostatic force is applied across the air gap which moves down the top mirror hence tuning the FP cavity thickness. The resulting FP mode resonance drift will cause the spectral overlap variation, thus the coupling strength.

Secondly, the PCM can be displaced inside the structure to adjust the field overlap between the PCM and FP cavity modes. In this case, both low index gap media must be in air to provide free released PCM [Fig. 2(b)]. The PCM position control can be achieved using two "head to tail" p-i-n junctions [13] electrostatic actuator as represented in Fig. 2(b). When biasing the global vertical structure, up or down PCM displacement is produced while keeping the device physical thickness. The PCM resonator can be translated therefore between a node and an anti-node position of the FP field, hence adjusting the field overlap. More specifically the splitting Δf is zero (resp. maximum)

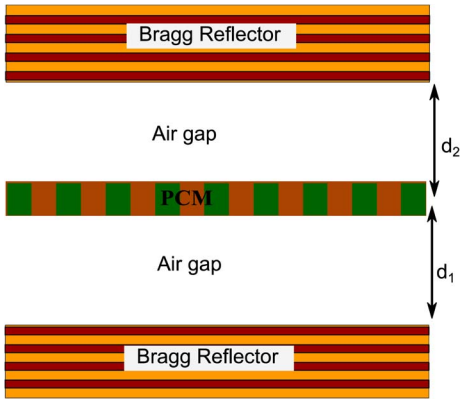

Fig. 3. Schematic cross view of the dual-wavelength micro-cavity formed by two quarter-wave Bragg reflectors FP cavity and a 1D PCM resonator.

when the field overlap integral of both modes is zero (resp. maximum) even under strong coupling regime.

3. Design of Tuneable Dual-Wavelength Micro-Resonator

3.1. Coupled Mode Theory Transfer Matrix Phenomenological Model

A PCM can be represented by a resonator, which can exchange energy with radiated modes propagating along the vertical direction. This interplay is defined by the resonance frequency and kinetics parameters, which describe the coupling rate between guided waves and free space modes. We may therefore combine coupled mode theory [19] and transfer matrix method to model the optical response of an arbitrary layers stack comprising PCM structures [1], [4].

We consider a basic air gap FP cavity with two quarter wave Bragg reflectors composed by 7 silicon/silica alternating layer stacks enclosing a PCM (Fig. 3.). The PCM will be accounted by a single punctual resonator with an even optical mode. For symmetric cavity, the splitting Δf is zero (resp. maximum) for wavelength (resp. half-wavelength) FP cavity [4], the spatial field overlap being zero (resp. maximum). The quality factor of the resonator $(Q_c = \omega_0 \tau_c/2)$ is chosen to assure strong coupling regime.

3.1.1. Tuning by Moving the top Mirror

A slight variation of the FP mode resonance around f_0 can be used to tune the coupling strength. The FP mode resonance variation lies on the cavity optical length modulation, obtained here by varying the top air gap thickness (Fig. 3.) through the upper mirror displacement. Fig. 4 shows the resonance wavelengths λ_1 and λ_2 and their quality factor evolution as a function of the top mirror displacement (δ) and depending on Q_c/Q_{FP} where Q_{FP} denominates the FP cavity quality factor. The FP cavity optical thickness is $d_0 = d_1 + d_2 = 1.5\lambda_0$ for $\delta = 0 (\delta = d_2 - 0.5d_0)$.

Fig. 4(a) demonstrates that the FP mode frequency control may help providing the frequency difference variation. Moreover, we observe that $\Delta\lambda = |\lambda_1 - \lambda_2|$ reaches minimum at the anti-crossing point where the PCM and FP cavity modes are perfectly tuned. Fig. 4(b) shows that far from the anti-crossing point, we obtain two independent resonances: a FP cavity mode that exhibits a finite quality factor and a second mode corresponding to the PCM mode with a quality factor tending to infinity as there is no output pathway for photons in this mode. Both resonances quality factors converge to the same value $Q = 2Q_{FP}$, regardless Q_c/Q_{FP} at the anti-crossing point. Let us notice here that the hybrid mode quality factor at the anti-crossing is twice the FP cavity one since they are equally shared between the PCM and the FP cavity parent modes [4]. We have reported previously [4] identical behavior of the micro-resonator with a very good agreement between the

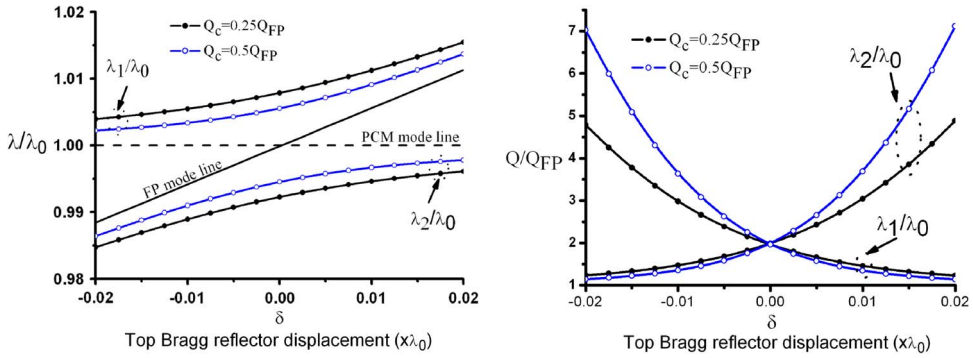

Fig. 4. Representation of the dual-wavelength micro cavity resonances (a) and their quality factor (b) variation as a function of the top mirror displacement $(\delta = d_2 - 0.5d_0)$.

phenomenological matrix method and 2D-FDTD simulations. Besides, the hybrid modes were found to be a linear combination of the PCM and FP parents' modes.

3.1.2. Tuning by Moving the Resonator Inside the FP Cavity

The basic idea of this tuning scheme is to preserve the frequency matching between the FP and the resonator to extend the hybrid modes tuning range. Indeed as the FP resonance is determined by the optical thickness of the micro-resonator and the PCM resonance is fixed by its structuration, the frequency matching should be remained while moving the PCM inside the structure. This is deemed to result in an improved control over the coupling strength of equal hybrid modes. Although exact FDTD simulations presented in the next section will show that this not fully true, the transfer matrix model well describes the optical characteristics of the micro-resonator under the resonator position variation.

The field overlap of the FP and the resonator modes depends on the resonator position in the cavity regarding the FP field distribution. A sine like evolution of the resonant frequencies versus the PCM position (δ) is expected therefore in accordance with the FP mode field distribution. Following our previous publication [4], the resonance frequencies separation can be estimated by Eq. (1), where $p\lambda_0$ is the cavity optical length and δ denotes the resonator position in the dual-wavelength micro-cavity

$$\frac{\Delta f}{f_0} = \frac{\Delta f_{max}}{f_0}\sin\left(\frac{2\pi}{\lambda_0}\delta\right) = \sqrt{\frac{2}{p\pi Q_c}}\sin\left(\frac{2\pi}{\lambda_0}\right). \quad (1)$$

To get a higher tuneability, the initial position $(\delta = 0)$ of the PCM is chosen to correspond to a zero frequency splitting. Hence, for small δ, Δf is a linear function of the resonator displacement.

Fig. 5. shows the resonance wavelengths and their quality factor evolution, for a λ_0 thick FP cavity and for two different sets of Q_c, as a function of the resonator position (δ) in the cavity. As expected, we observe that the resonance frequency variation mimics the FP field distribution with a node (zero splitting) at the center of the cavity. Consequently, the full tuning range, which is set by Q_c, is achieved for a 0.25 λ_0 displacement of the resonator.

The quality factor of both resonant frequencies is almost the same (about twice Q_{FP}). However, it appears that the resonator displacement leads to a weak perturbation effect which unbalances slightly the quality factors as the resonator is moved from the structure center. The hybrid modes exhibit notwithstanding a very good sharing of parent modes, in sharp contrast with previous tuning scheme, where the top reflector of the cavity is moved.

3.2. Numerical FDTD Simulation Validation

Based on the phenomenological matrix transfer results presented above, we design a tuneable dual-wavelength micro-resonator using numerical 2D-FDTD simulation. The tuning by moving the

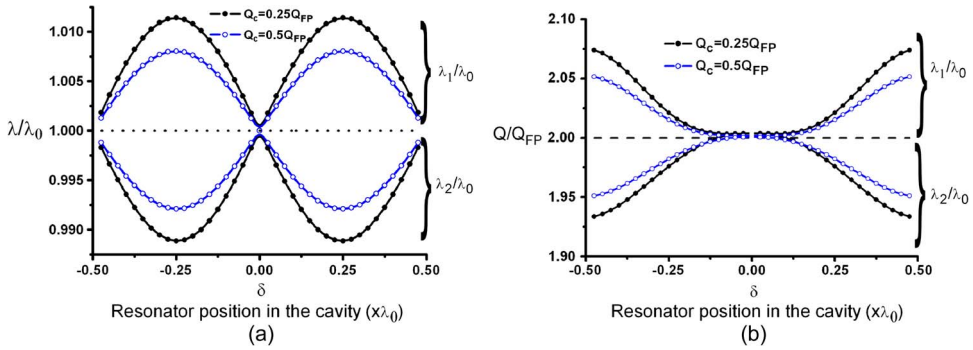

Fig. 5. Hybrid mode resonance wavelengths (a) and their quality factors (b) evolution as a function of the resonator position.

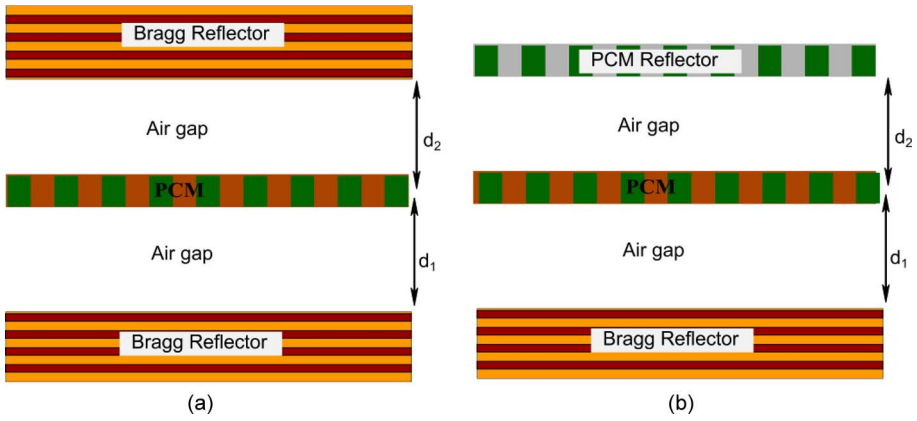

Fig. 6. Schematic representation of dual-wavelength resonant micro-cavity combining a PCM resonator and (a) two DBR reflectors FP cavity or (b) a FP cavity formed by a DBR and a PCM reflectors.

top mirror simply amount to the FP cavity thickness variation around the anti-crossing point. In that case, we reported identical result to Fig. 4 in previously paper with a good agreement between the phenomenological matrix model and the 2D-FDTD simulation [4]. Hence, in this section, we main focus on the tuning by the PCM resonator displacement inside the FP cavity only. Fig. 6(a) depicts a coupled PCM resonator and two quarter-wave Bragg reflectors FP cavity structure. And, as an alternative to improve the device compactness, we use a PCM reflector instead of a thick Bragg stack. Therefore, we consider also a second design architecture as shown in Fig. 6(b) where the FP cavity is formed by a bottom quarter-wave Bragg reflector and a top PCM mirror [15], [16].

Only 1D grating structure and TE polarization (electric field is along the slit axis) are considered in this work, but the concept can be easily extended to TM modes and 2D gratings. The PCM resonator consists in a 1D lattice of slits drilled in 0.25 μm thick InP membrane $(n = 3.17)$ with air cladding on both sides. The lattice period is $T_{PCM} = 0.8$ μm and the air slit filling factor is 26%. The PCM reflector consists in a 1D lattice of slits drilled in 0.35 μm thick InP membrane with a period of $T_{RPCM} = 1.2$ μm and an air slit filling factor of 75%. Note that the resonator and the reflector PCMs' period ratio is rational $(T_{TRPCM}/T_{PCM} = 1.5)$. This allows us further to use periodic boundary conditions for FDTD simulation in the Fig. 6(b) design case. The Bragg reflector consists in four (4) bi-layer quarter-wave stack of silicon and silica. To determine the spectral characteristic of each element and of the dual-wavelength micro-resonator, a plane wave time pulse is launched at their top surface at normal incidence. Fourier transform of the temporal recording of the reflexion and transmission detectors is performed at the end of each simulation to provide the spectral response.

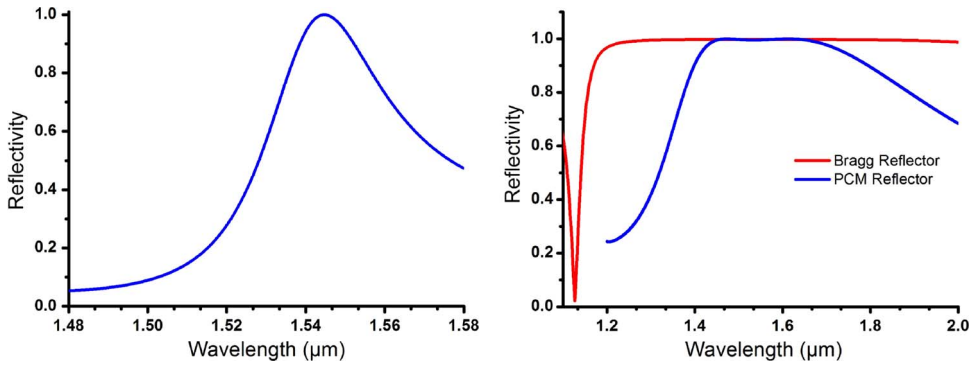

Fig. 7. (a) PCM resonator and (b) PCM and Bragg reflectors reflectivity spectrum under a TE-polarized plane wave normal incidence.

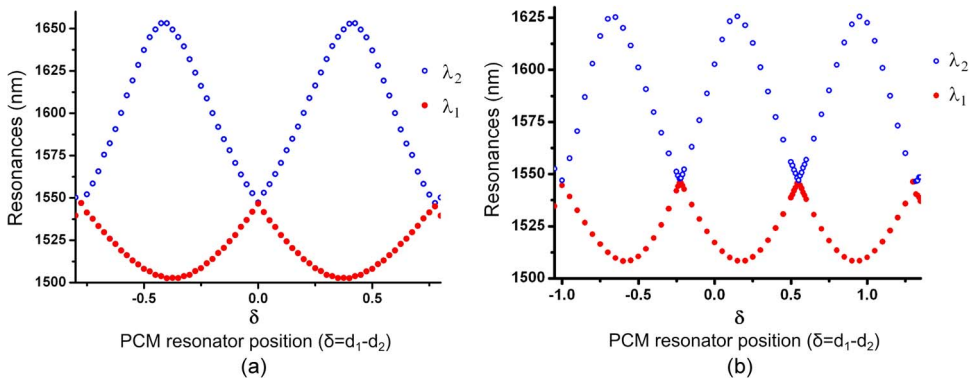

Fig. 8. Hybrid modes resonance wavelengths variation as a function of the resonator position in the FP cavity. ($\delta = 0$ stand for equal air gap aside the PCM resonator). (a) and (b) correspond, respectively, to a design of Fig. 6(a) and (b).

Periodic boundary conditions is assumed along the horizontal axis when perfectly matched absorbing layers (PML) are applied at the end of the simulation domain in the vertical direction to simulate free space propagation.

The reflection spectra of the PCM resonator, the PCM and the Bragg reflectors are plotted in Fig. 7. The PCM resonator exhibits a resonant mode at $\lambda_0 = 1545$ nm [Fig. 7(a)] with large line-width. A low quality factor (large line-width) resonator is preferred to provide easily a strong coupling regime [4] and a large tuning range [Eq. (1)]. In Fig. 7(b) we can see that high efficient mirrors are provided by both the PCM and the Bragg reflectors. The reflectivity is larger than 99% over 1450 nm to 1650 nm wavelength range for the PCM reflector and over 1250 nm to 1970 nm range for the Bragg reflector.

Fig. 8(a) and (b) show the resonance frequencies evolution as functions of the PCM resonator displacement (δ) corresponding respectively to the design of Fig. 6(a) and (b). $\delta = 0$ stands for equal air gaps and negative abscissa correspond to a displacement toward the bottom Bragg reflector. The total air gaps thickness is 2450 nm in case of Fig. 8(a). and 2900 nm in case of Fig. 8(b). The air gap thickness difference, in both designs, is linked to reflectivity phase difference between the Bragg reflector and the PCM mirror. Besides, as the design is no longer physically symmetric in Fig. 6(b), the frequency splitting at the origin [Fig. 8(b)] is neither zero nor maximum.

In both design simulations, we observe a periodic (sinusoidal) variation of the resonance frequencies as expected according with previous phenomenological matrix model observations. The wavelength difference maximum tuning is 150 nm (resp. 115 nm) for a PCM displacement over 350 nm (resp. 325 nm) in Fig. 6(a) [resp. Fig. 6(b)]. They correspond respectively to an

average optomechanical coupling efficiency of 0.124 THz/nm and 0.095 THz/nm. It can be noticed that the PCM overall displacement is close to 0.25 λ_0 in both cases for the maximum frequency difference.

However, we note clearly, unlike the model [Eq. (1)], a different amplitude variation for both wavelengths in Fig. 8. This difference can be explained by the perturbation, caused by the PCM displacement, on the FP mode. Indeed, this displacement changes not only the field overlap of the FP and PCM modes but also the FP resonance frequency itself [8]. This results in a spectrally detuned PCM and FP cavity system which leads to the asymmetric evolution of the resonance wavelengths. Under these conditions, the hybrid modes balance only where the FP and PCM parent modes matched perfectly, that is to say in the immediate vicinity of the central wavelength λ_0. Elsewhere, the highest amplitude variation mode has a larger FP component weight than the other and conversely. Such FP resonance frequency drift effect, cause of the PCM displacement, has not been included in the phenomenological matrix model where we used a point resonator. Notwithstanding, the phenomenological model properly describes the dual-wavelength micro-resonator behavior under tuning by the PCM displacement as confirmed by FDTD simulations.

We must caution reader here that the results presented above in Sections 3.1 and 3.2 assume an ideal and laterally infinite component. In practice for a real device with fixed dimensions, we may account additional losses as photon lateral loss or manufacturing imperfection losses. These losses can influence the localization and the quality factor of the resonance frequency of the PCM membrane and FP cavity, therefore those of the hybrid modes.

The fabrication of such tuneable dual-wavelength micro-cavity is in progress in our institute. It is a matter of micro-fabrication to integrate a PCM inside a vertical cavity [20] which should be combined with our PC-MOEMS processing technology [12], [21] in order to provide movable suspended membranes. In brief, the fabrication of a tuneable dual-wavelength micro-cavity involve key technological steps including: high index contrast Si/SiO_2 Bragg reflector deposition, epitaxy of III-V InP based quantum hetero-structures to provide optical gain for laser emission, nano-patterning of the InP-based membrane (PCM), membrane bonding and selective micromachining. Strain relaxation in suspended microstructures has to be taken into account and specific mechanical and geometrical engineering should be then applied by designing adapted pre-stressed layers and platforms.

4. Conclusion

Phenomenological coupled mode theory and numerical 2D-FDTD simulations have been used in this work to demonstrate a novel compact and tuneable dual-wavelength optical micro resonator design combining a photonic crystal membrane and a vertical Fabry–Perot cavity. The dual-wavelength micro-resonator architecture is full described and the tuneability options are presented. The dual-wavelength resonances arise from a strong optical coupling between a PCM resonator Γ–point Bloch mode and a vertical resonant FP cavity mode with same frequency. Hence, we may provide tuneability by controlling such a coupling strength through coupling conditions variation, i.e., the spectral and the field overlaps of both modes.

Both coupling conditions control have been considered individually in the case of phenomenological model analysis while it turns out that the field recovery control is always been accompanied by a spectral matching variation with numerical FDTD simulation. However, as predicted by analytical study [Eq. (1)], we demonstrate in both cases that the PCM displacement over 0.25 λ_0 covers all tuning range due to the FP field periodicity. In our work, a maximum tuning range of about 150nm has been achieved numerically with a dual-wavelength micro-resonator of 2 λ_0 total optical length.

It is worth noticing that our design is not only suitable to provide two resonant modes but also to control their spectral and polarization properties. Further, we have described in our previous work [2], [12], [20], [21], processes which can give rise to such 2.5D micro-photonic devices and consequently paving clearly the way for new optical functionality exploration in a vertical micro-cavity.

References

[1] X. Letartre, J. Mouette, J. L. Leclercq, P. Rojo Romeo, C. Seassal, and P. Viktorovitch, "Switching devices with spatial and spectral resolution combining photonic crystal and MOEMS structures," *J. Ligthw. Technol.*, vol. 21, no. 7, pp. 1691–1699, Jul. 2003.

[2] J. L. Leclercq, P. Rojo-Romeo, C. Seassal, J. Mouette, X. Letartre, and P. Viktorovitch, "3D structuring of multilayer suspended membranes including 2D photonic crystal structures," *J. Vac. Sci. Technol. B*, vol. 21, no. 6, pp. 2903–2906, Nov. 2003.

[3] B. Ben Bakir, C. Seassal, X. Letartre, P. Viktorovitch, M. Zussy, L. Di Cioccio, and J. M. Fedeli, "Surface-emitting microlaser combining two-dimensional photonic crystal membrane and vertical Bragg mirror," *Appl. Phys. Lett.*, vol. 88, no. 8, pp. 081113-1–081113-3, Feb. 2006.

[4] K. Kusiaku, O. El Daif, J. L. Leclercq, P. Rojo-Romeo, C. Seassal, P. Viktorovitch, T. Benyattou, and X. Letartre, "Dual-wavelength micro-resonator combining photonic crystal membrane and Fabry–Perot cavity," *Opt. Express*, vol. 19, no. 16, pp. 15 255–15 264, Aug. 2011.

[5] D. Gusev, I. Soboleva, M. Martemyanov, T. Dolgova, A. Fedyanin, and O. Aktsipetrov, "Enhanced second-harmonic generation in coupled microcavities based on all-silicon photonic crystals," *Phys. Rev. B*, vol. 68, no. 23, pp. 233102-1–241102-3, Dec. 2007.

[9] M. Tani, P. Gu, M. Hyodo, K. Sakai, and T. Hidaka, "Generation of coherent terahertz radiation by photomixing of dual-mode lasers," *Opt. Quantum Electron.*, vol. 32, no. 4/5, pp. 503–520, May 2000.

[10] P. M. Osterberg, "Electrostatically actuated micreoelectromecahnaical test structures for material property measurement," Ph.D. dissertation, Mass. Inst. Technol., Cambridge, MA, USA, 1995.

[11] M. Strassner, J. Daleiden, N. Chitica, D. Keiper, B. Stalnacke, S. Greek, and K. Hjort, "III–V semiconductor material for tuneable Fabry–Perot filters for coarse and dense WDM systems," *Sens. Actuators*, vol. 85, no. 1–3, pp. 249–255, Aug. 2000.

[12] S. Boutami, B. Ben Bakir, J.-L. Leclercq, X. Letartre, P. Rojo-Romeo, M. Garrigues, and P. Viktorovitch, "Highly selective and compact tuneable MOEMS photonic crystal Fabry–Perot filter," *Opt. Express*, vol. 14, no. 8, pp. 3129–3137, Apr. 2006.

[13] M. Garrigues, J. Danglot, J. L. Leclercq, and O. Parillaud, "Tuneable high-finesse InP/air MOEMS filter," *IEEE Photon. Technol. Lett.*, vol. 17, no. 7, pp. 1471–1473, Jul. 2005.

[14] K. S. Yee, "Numerial solutions of initial boundary value problems involving maxwell's equations in isotropic media," *IEEE Trans. Antennas Propag.*, vol. AP-14, no. 3, pp. 302–307, May 1966.

[15] C. Chang-Hasnain, C. Mateus, and M. Huang, "Ultra broadband mirror using subwavelength grating," U.S. Patent 7 304 781, Dec. 4, 2007.

[16] S. Boutami, B. Ben Bakir, H. Hattori, X. Letartre, J.-L. Leclercq, P. Rojo-Romeo, M. Garrigues, C. Seassal, and P. Viktorovitch, "Broadband and compact 2-D photonic crystal reflectors with controllable polarization dependence," *IEEE Photon. Technol. Lett.*, vol. 18, no. 7, pp. 835–837, Apr. 2006.

[17] P. Vincent and M. Neviore, "Corrugated dielectric waveguides: A numerical study of the second-order stop bands," *Appl. Phys.*, vol. 20, no. 4, pp. 345–351, Dec. 1979.

[18] R. Magnusson and S. S. Wang, "New principle for optical filters," *Appl. Phys. Lett.*, vol. 61, no. 9, pp. 1022–1024, Aug. 1992.

[19] C. Manolatou, M. J. Khan, S. Fan, P. R. Villeneuve, H. A. Haus, and J. D. Joannopoulos, "Coupling of modes analysis of resonant channel add–drop filters," *IEEE J. Quant. Electron.*, vol. 35, no. 9, pp. 1322–1331, Sep. 1999.

[20] K. Kusiaku, J. L. Leclercq, P. Regreny, P. Rojo-Romeo, C. Seassal, P. Viktorovitch, X. Letartre, L. Chusseau, F. Disanto, F. Philippe, and E. Augendre, "Dual-wavelength laser for THz generation by photo-mixing," in *Proc. SPIE*, 2012, vol. 8425, pp. 84250H-1–84250H-8.

[21] S. Boutami, B. B. Bakir, J.-L. Leclercq, X. Letartre, C. Seassal, P. Rojo-Romeo, P. Regreny, M. Garrigues, and P. Viktorovitch, "Photonic crystal-based MOEMS devices," *IEEE J. Sel. Topics Quantum Electron.*, vol. 13, no. 2, pp. 244–252, Mar./Apr. 2007.